Minefill 2020-2021 – Hassani et al (eds)

Paste-waste design and implementation at Newmont Goldcorp's Tanami Operation

Ryan L. Veenstra & Johannes J. Grobler
Newmont Goldcorp Australia

SUMMARY: Newmont Goldcorp's Tanami Operations consists of the Dead Bullock Soak underground mine (DBS) and the Granites Processing Plant. DBS is currently undergoing an expansion which has created a surplus of underground (UG) waste rock. In order to deal with this surplus of waste rock a paste-waste project was initiated. The goal of this project was to develop and implement a design methodology of maximizing waste rock disposal by depositing the waste rock in primary stopes (usually only filled with 100% cemented paste backfill [CPB]). This paper presents the details of how the design methodology was developed. This includes an analysis of rock chute placement, waste rock versus CPB fill rates, and backfill strength design. Finally, the paper also presents a case study of a paste-waste stope. This study includes an economic analysis of paste-waste, highlighting the importance of paste-waste to DBS in the future.

Keywords: Paste Waste, Cemented Paste Backfill, Design, Stability

1 INTRODUCTION

The Dead Bullock Soak (DBS) underground (UG) mine at Newmont Goldcorp's Tanami Operation (NGT) is expanding to be able to mine deeper and more laterally distance stopes. In order to excavate these stopes, the amount of UG development (i.e. access tunnels to get to the stopes) will also increase, causing a subsequent increase in waste rock (WR).

The DBS mine currently operates in a primary-secondary sequence, with the primaries being filled with cemented paste backfill (CPB) and the secondaries with WR. Due to the expansion, there is not enough secondary stope void to accommodate the WR being generated. Figure 1 shows the life-of-mine (LOM) WR profile. This figure compares the amount of WR that is generated (green column) and the amount of WR void available (red column). The difference (blue columns) between these values is the amount of WR that will need to be trucked to surface. This figure shows that there will be a surplus of WR generated over the next 7 years. In order to reduce the amount of WR transported to surface, a project was initiated to increase the amount of WR being deposited UG. Part of this project was building on DBS's current paste-waste (PW) processes. PW is defined a process that backfills a stope with both CPB and WR.

2 PASTE-WASTE METHODOLOGY

PW backfill masses have been placed at DBS for several years in the form of CPB plugs or caps. However, these were generally secondary stopes that would be undercut or required tight filling. In order to increase the amount of PW, a different methodology was required.

DOI: 10.1201/9781003205906-34

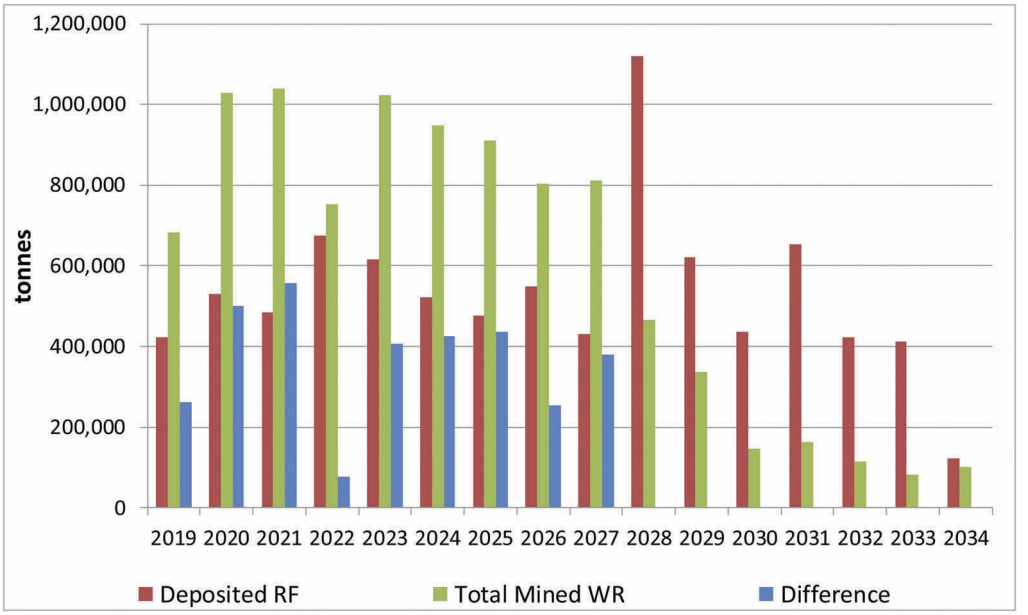

Figure 1. Graph presenting the LOM waste rock balance.

The PW method needed to rely on WR being dumped into the stope via the UG trucking fleet. The majority of the run-of-mine waste rock is too large to reticulate. Figure 2 contains the particle size distributions (PSD) for the current tailings blend being used for CPB production, the run-of-mine WR, and the raise bore fines. The dashed vertical line is a rule-of-thumb for the maximum particle size that could be transported by the DBS reticulation system. Any screening or crushing process to reduce the WR to the required size was unfeasible.

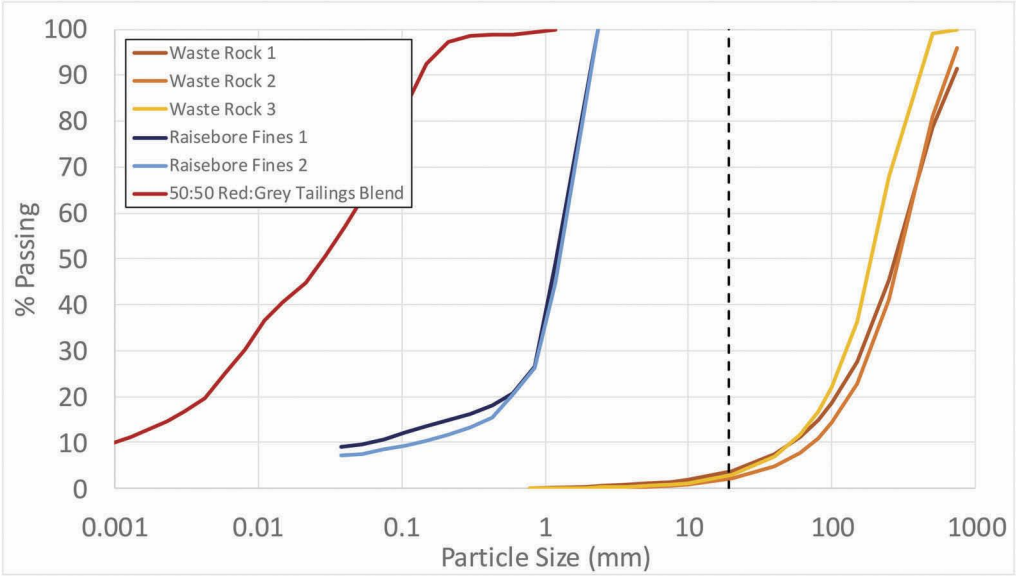

Figure 2. Particle size distributions for onsite backfill materials.

Given the truck dumping requirement, it was decided to pursue an 'encapsulation' type of filling method. In this method, the waste is isolated from an exposure surface by being encapsulated completely by the CPB. The amount of WR that can be deposited using this method varies considerably on the number of vertical exposures and the dumping location.

Figure 3 highlights the difference in the amount of WR that can be deposited into the same sized stope with four vertical exposures versus two touching vertical exposures. Note that if the two exposure surfaces were opposite to each other the amount of deposited WR would be the same as the four-exposure stope.

Figure 4 highlights the difference that the deposition location makes to the amount of WR that can be placed into the same sized stope given. The central diagram represents an end-dump type of deposition while the right-hand diagram would require a rock chute. The left-hand diagram could be either an end-dump or a rock chute depending on the access drive and stope geometries. In order to determine a mass balance and stope stability, it is necessary to determine the location of the WR within the stope.

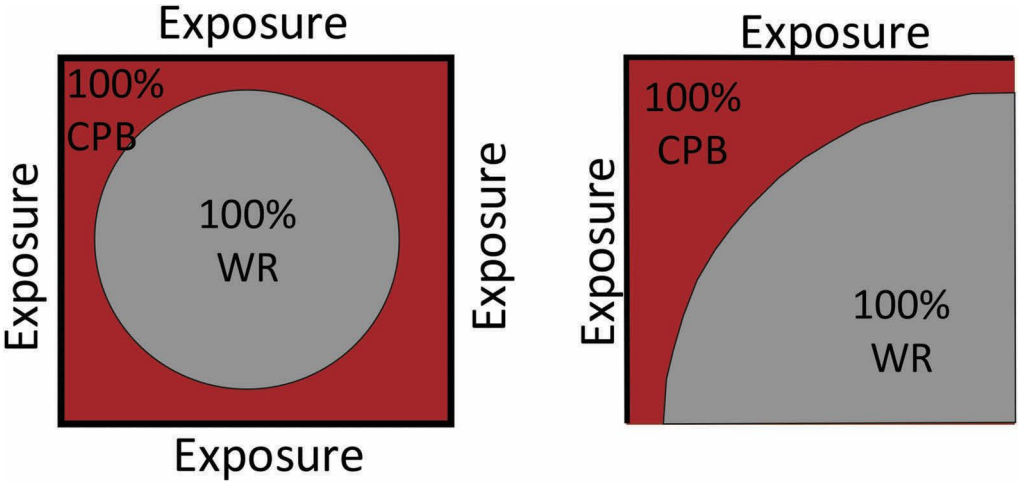

Figure 3. Difference in WR deposition due to increased exposure surfaces.

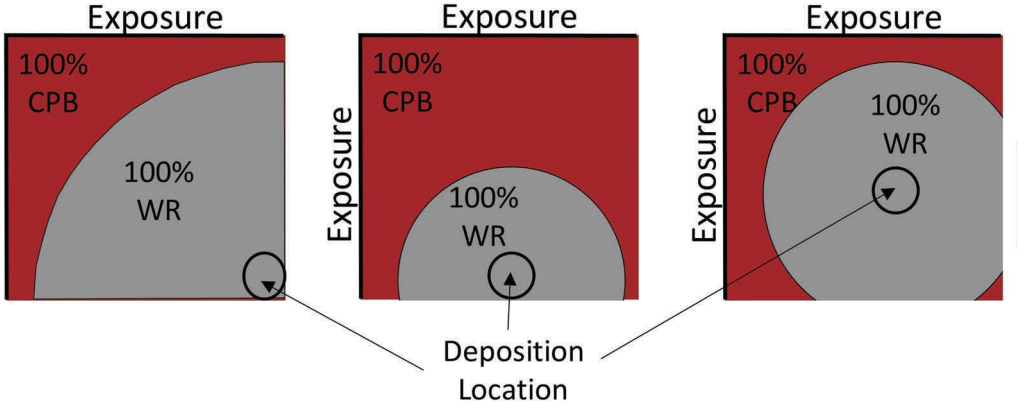

Figure 4. Difference in WR deposition due to different deposition locations.

2.1 *Segregation modelling*

Segregation modelling refers to determining the position of the WR within the stope. Segregation modelling has two parts. The first part was determining where the WR would be deposited in the stope while the second was to determine what the shape of the WR would be within the stope.

2.1.1 *Deposition location of waste rock*

Determining the location of the WR profile was accomplished by using Trajec3D (Basrock, 2019). This freeware program was originally designed for rock fall analysis for open pit walls but has also been used to show material flow within a stope (Basson et. al., 2015).

Figure 5 a) and b) show two examples of a calibration exercise conducted comparing the surfaces of deposited WR, as determined by cavity monitoring surveys (CMS), with the flow trajectory predicted by Trajec3D. The CMS surveys agree well with the modelled locations. Figure 5 c) shows a modelled flow trajectory for an angled rock chute.

2.1.2 *Waste rock shape determination*

The shape of the WR depends on the deposition rates of the CPB and WR within the stope, the shape of the stope, and deposition location. If both deposition rates are kept constant and

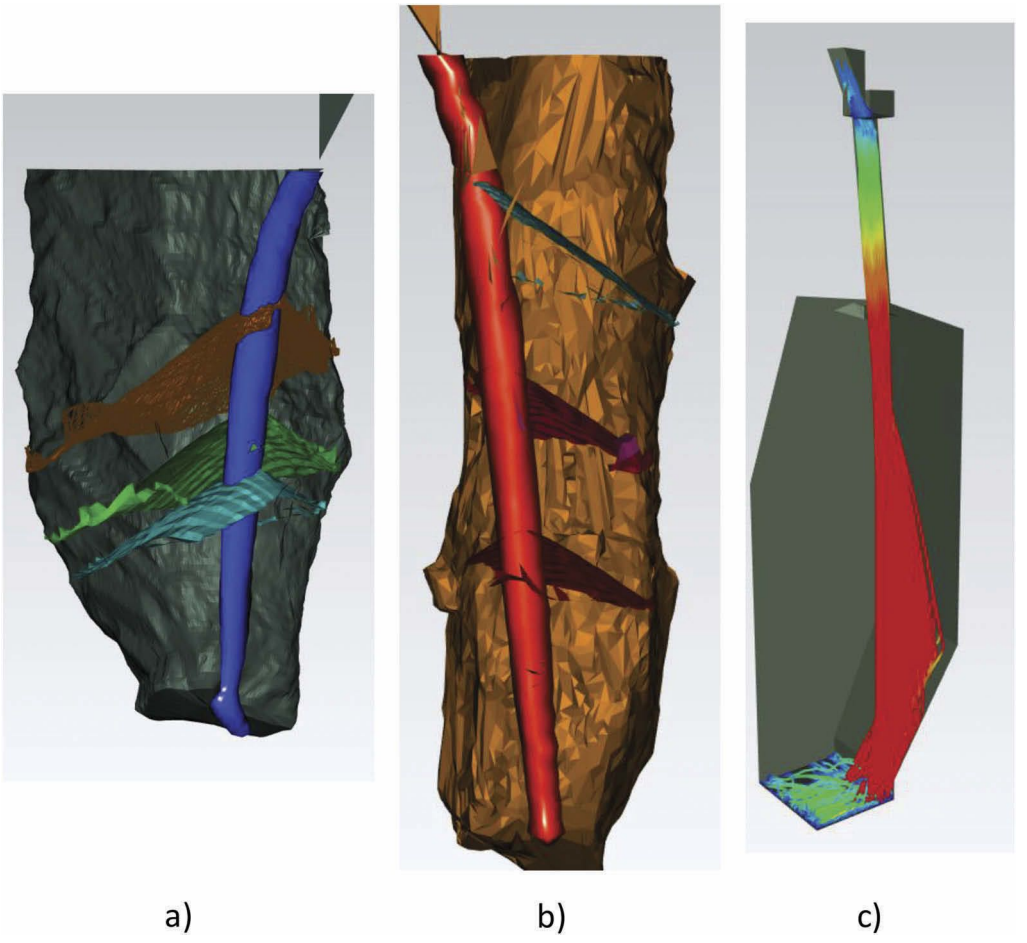

Figure 5. Trajec3D results compared to CMS data for a) a double lift end-dump and b) a triple lift end dump, and c) a Trajec3D model single lift angled rock chute.

are deposited into a uniform shaped stope then the backfill rise-rate will eventually stabilize to a continuous rate. The backfill rise-rate is the height of the CPB level including the WR within it.

This is shown schematically in Figure 6, where the initial WR cone volume is small. This means that the CPB has a large volume to fill, causing the small combined backfill rise-rate. With subsequent WR deposition, the rate-of-change of the WR volume becomes negligible and the backfill rise-rate stabilizes. Figure 6 also introduces the concept of a WR halo. Essentially this halo is a transition zone between the 100% WR section inside stope and the 100% CPB encapsulating it. Currently, the size of the halo (or even if a halo exists) is unknown. Conservatively, the size of the halo was determined to be the radius of the WR cylinder plus twice the length of the isolated section of each WR cone (as shown in Figure 6).

However, the above deposition model is unrealistic as stopes are not uniformly shaped and the deposition rates, particularly the WR rates, are not constant. The inconstant nature of the WR deposition is due to when the WR trucks are available. In order to deal with this inconsistency, the design was initially bookended by a 'staggered' or an 'instantaneous' design. The staggered approach mean that each truck was deposited at equal-time intervals over a shift whereas the instantaneous approach meant that the entire amount of deposited WR for the shift was deposited instantaneously once during the shift.

An algorithm was developed on-site accounting for the volume changes within the stope as well as the CPB and WR deposition rates. This allowed the size of the WR cylinder and halo to change with changing stope volume. Essentially, a decrease in stope volume caused the WR cylinder to increase while an increase in stope volume caused a decrease. There are limitations

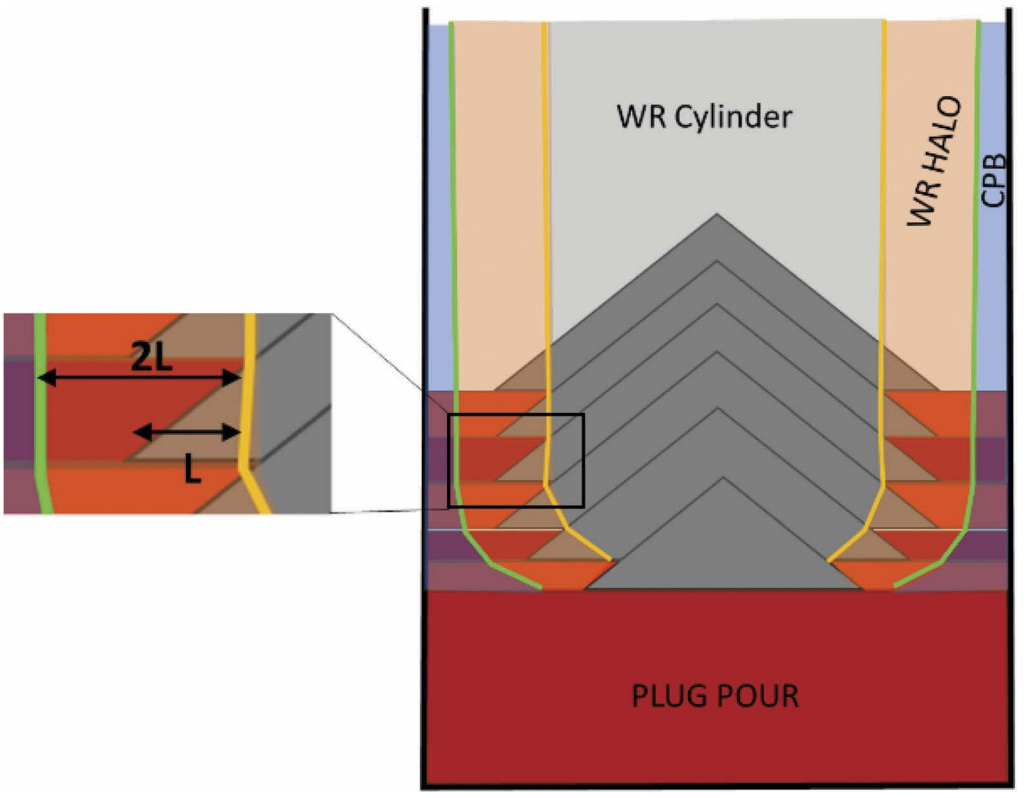

Figure 6. Schematic of the encapsulation model delineating the WR cylinder, WR halo, and CPB areas.

to the algorithm as it works best when the entire WR volume is encapsulated within the stope volume (e.g. the 4-sided exposure schematic in Figure 3). Algorithm variations have been trialled using half or quarter volume cones but these require stopes with relatively straight sides and/or a 90° corner.

An example of the results of this algorithm are shown in Figure 7. This graph shows the results of a staggered versus instantaneous design analysis by plotting WR radius versus back-fill height. The volume of the stope with height is also shown. A comparison of the WR radius to stope volume line confirms the stope volume to WR radius relationship discussed above.

Figure 7 also shows the staggered model tends to have smaller cylinder and halo sizes but more irregular curves. This is due to resolution issues within the algorithm. Therefore, the instantaneous values were used for stability analysis as this was considered a worst-case scenario.

Figure 8 shows a comparison of the algorithm's results to those of Deswik.CAD's backfill simulator for an instantaneous condition (Deswik, 2019). There was excellent correlation between the two. Unfortunately, the Deswik.CAD analysis took over 5 hours to run which was substantially slower than the site-developed algorithm. However, for more complex

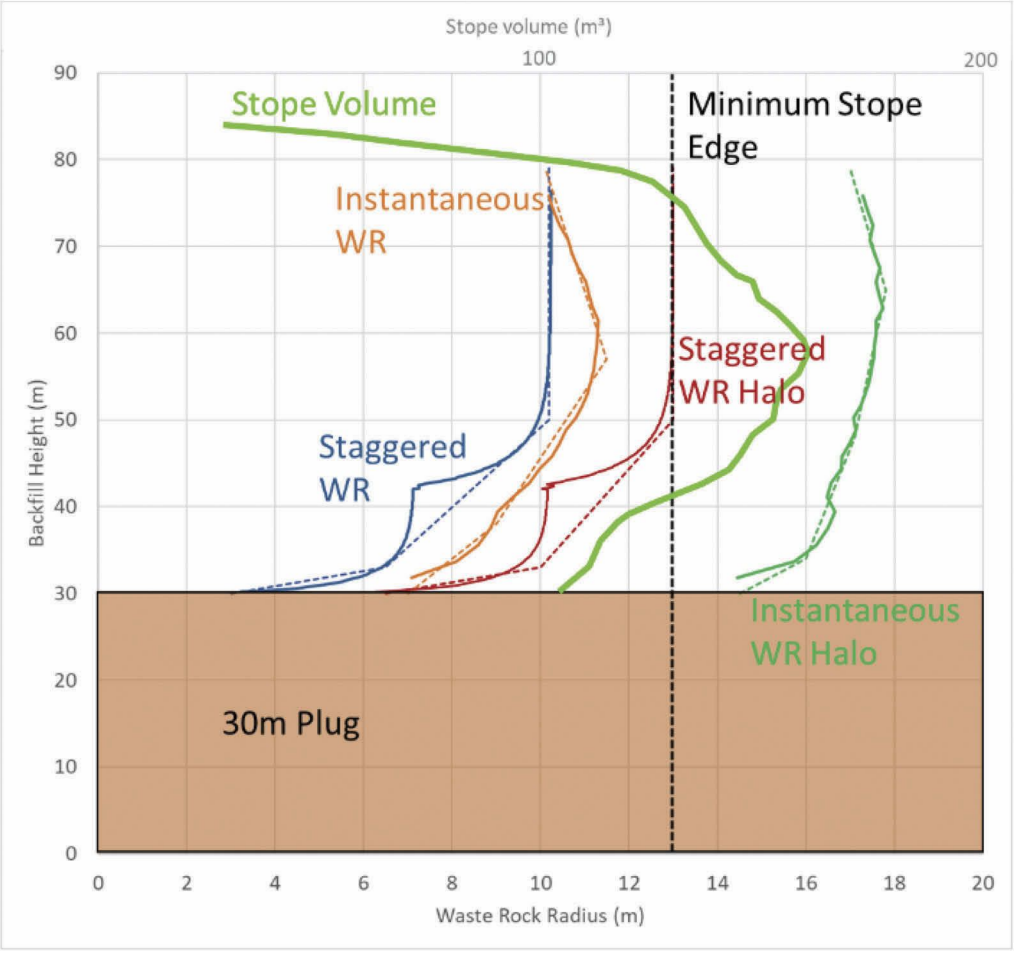

Figure 7. WR size algorithm results comparing a staggered and instantaneous design. The stope volume is also shown.

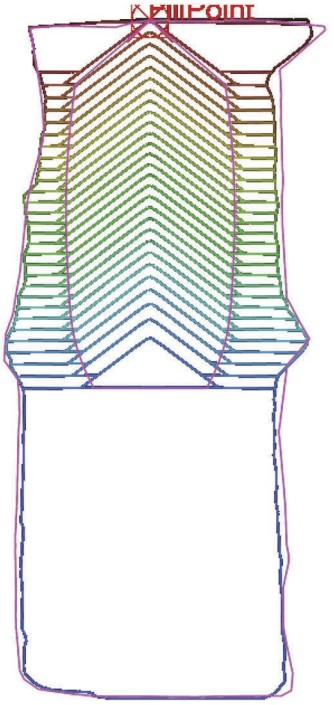

Figure 8. Comparison of WR volume determined by site algorithm (magenta) and Deswik.CAD.

volume relationships (i.e. the WR volume is not enclosed and cannot be approximated using half or a quarter of cone volume) then using Deswik.CAD would be required.

2.2 *Stability modelling*

The stability modelling was completed using Itasca's Flac3D software (Itasca, 2019). This software has a built-in factor of safety (FOS) solver. This solver uses a strength reduction method that modifies the input strength parameters (primarily cohesion and friction angle but can include other parameters such as tensile strength, dilation angle, etc.) by using a safety factor. The equations for the cohesion and friction angle reductions are below, where ϕ is the friction angle and F^{trial} is the safety factor:

$$cohesion^{trial} = \frac{cohesion}{F^{trial}} \tag{1}$$

$$\phi^{trial} = arctan\left(\frac{\tan\ \phi}{F^{Trial}}\right) \tag{2}$$

The program brackets the minimum safety factor by running a series of models at different safety factors. The solver stops when the minimum safety factor has been determined.

2.2.1 *Modelling inputs*

The basic parameters for any Flac3D model are density, elastic modulus, and Poisson's ratio. The use of an additional failure criterion requires further strength-related parameters. In this methodology, the Mohr-Coulomb failure criterion was used. The cohesive strength, friction angle, and tensile strength were incorporated in that criterion.

Most CPB testing programs involve determining the unconfined compressive strength (UCS) of the CPB with time. For this work, inputs were required for the WR and the WR halo zones. The WR inputs were determined from shear box tests but the WR halo inputs were more difficult to determine.

In order to obtain a better understanding of the strength parameters, above what UCS testing can provide, multiple consolidated undrained (CU) triaxial tests were undertaken of both the 100% CPB as well as various mixes of CPB and raise bore fines (RBF). These RBF mixes were intended to represent the mixing between the CPB and WR. RBF were used as they were small enough to be added to casting cylinders (PSDs of the RBF are shown in Figure 2).

Figure 9 shows the cohesion, UCS, elastic modulus, and friction angle curves for the RBF mixes, which were normalized to 100% CPB control tests. Multiple curing ages and binder contents were included in this plot and, while there is some scatter, there are some general trends. Essentially, the friction angle increases with increased addition of RBF, while the cohesion, UCS, and elastic modulus decrease. It was decided to use a 50:50 CPB to RBF ratio for determining the strength of the halo material as this was assumed to conservative. The tensile strength of the CPB or halo was assumed to be ten percent of the material's UCS.

2.2.2 *Modelling results*

Figure 10 shows an example of the analysis completed using the FLac3D FOS solver. Figure 10 a) shows the results of a model with no encapsulated WR, generating a relatively small surface 'bowl' failure with a FOS of 2.1. Figure 10 b) shows the configuration of the WR and halo within the stope. Figure 10 c) shows the results from a model of the second section, generating a much larger, full body failure surface with a FOS of 1.87. Note that the CPB strength was not modified between the models.

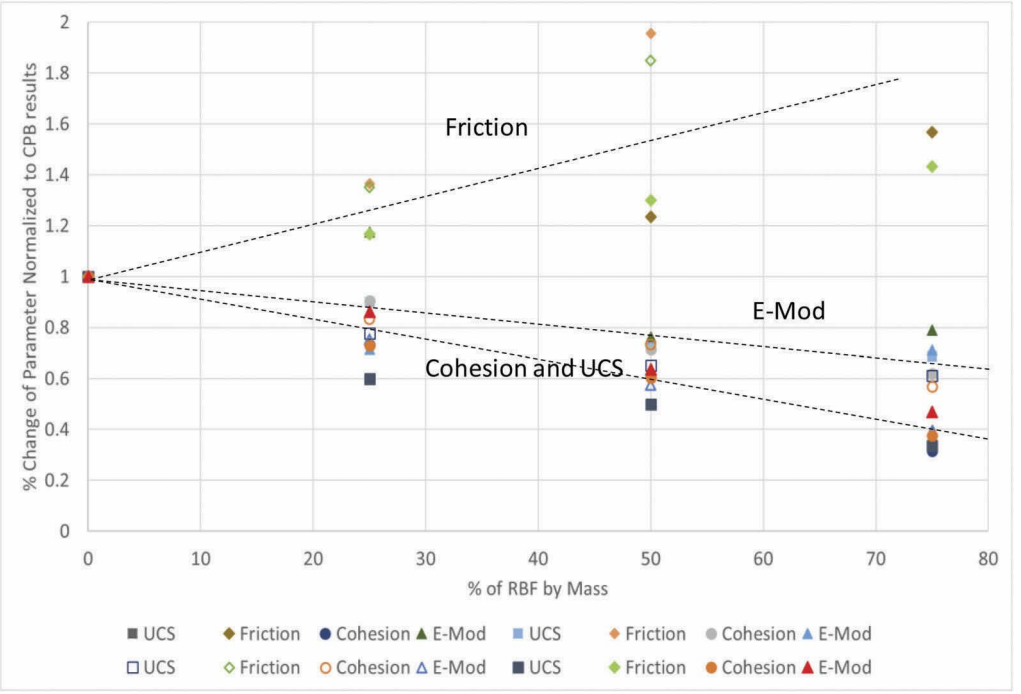

Figure 9. Normalized friction, cohesion, UCS, and elastic modulus curves in relation to increased RBF.

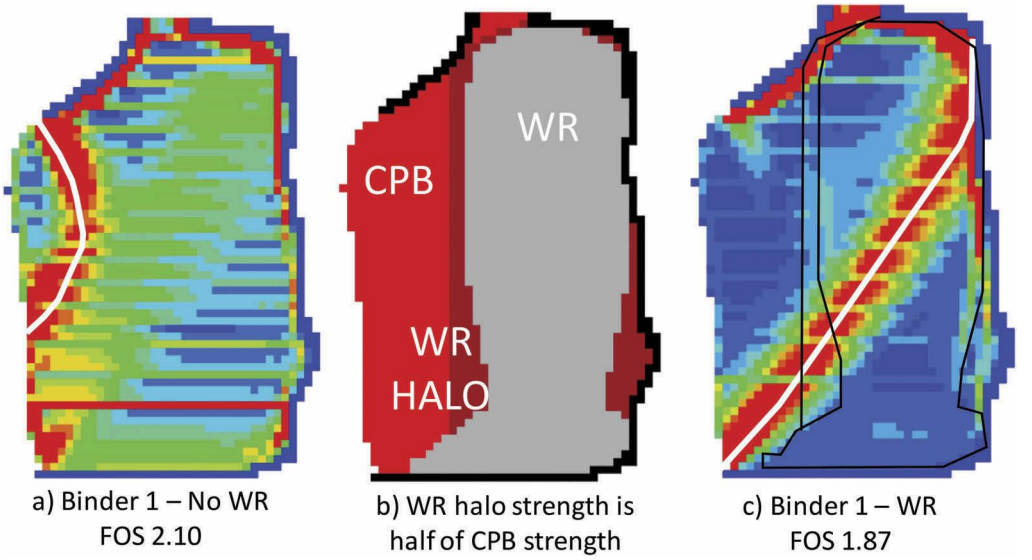

Figure 10. Stope sections showing the results for a model without the WR cylinder and halo, the locations of the added WR cylinder and halo, and the results of the model with the WR cylinder and halo.

2.3 *Methodology conclusions*

The methodology shown here provides framework by which an encapsulation paste-waste design can be completed and highlights the optimization that is allowed by this approach. It allows flexibility to the amount of WR that can be deposited in a stope by taking into account the operational or geometrical constraints. Additionally, the amount of binder required to produce a stable backfill mass can be optimized. Several key assumptions have been made in order to do this analysis:

1. There is a transition zone between the areas of 100% CPB and 100% WR
2. The strength of this transition zone can be approximated by the RBF strength testing
3. That using the 50:50 CPB/WR strength ratios are a worst-case scenario

Future work is planned to determine the validity of these assumptions.

3 CASE STUDY – 085A STOPE

The 085A was the first PW stope to be filled using the methodology discussed in Section 2. The stope was located approximately 800 m below surface in the Upper Auron portion of the DBS mine. It was a double-lift primary stope that was scheduled to be completely filled with CPB. The stope will be exposed vertically on its east and west sides and has a horizontal 'ledge' exposure. These are shown in the right-hand drawing in Figure 11. The exposures are numbered in the sequence that they were to occur.

The upper level access drive was undercut which required the WR to be deposited through a rock chute from the level above the stope. However, the CPB was able to be deposited into the stope from the upper level access drive. The rock chute was designed to be vertically inclined.

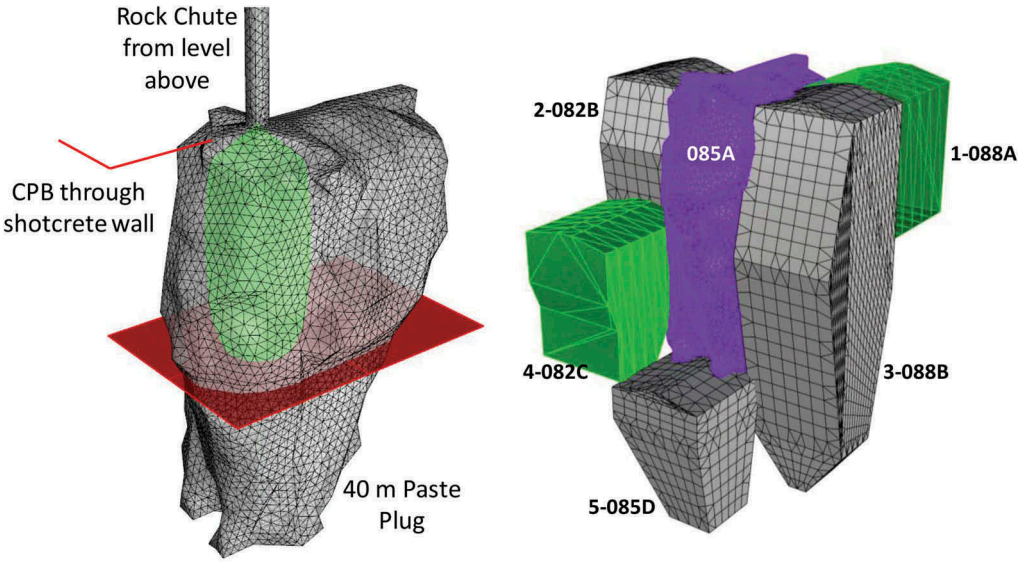

Figure 11. Drawings showing a) the 085A filling locations and the shape of WR cylinder, and b) the backfill exposures.

3.1 *Design*

The initial design had the PW process starting once an initial 15 m plug was installed. The plug was designed to deal with the 'ledge' exposure. However, due to operational demands, the first lift was completely filled with CPB.

The WR deposition rate targeted was 12 trucks per shift, which works out to approximately 1,400 tonnes per day, an amount that accounts for approximately 70% of DBS's total daily WR deposition. The onsite algorithm was used to determine the shape of the WR cylinder based on the location of the rock chute (green cylinder in Figure 11). Note that a Trajec3D model (Section 2.1.1.) was not completed for this stope as part of the initial design.

The design was further refined to determine the total of amount of WR and CPB that would be placed into the stope and the expected filling times. These plots are show in Figure 12. The total stope void (above the initial plug) was approximately 62,000 m³, of which the WR was going to account for approximately 18% (or 11,000 m³). There was also an expected 4-day decrease in filling time due to PW of this stope.

The stability analysis indicated that the third exposure (088B stope) was the critical exposure and the binder content was modified to achieve a FOS of 2. This minimum FOS was determined from a previous calibration exercise undertaken by DBS backfill personnel (Veenstra, 2019). Figure 13 shows a graph of the binder contents with height. The blue line represents the binder content determined from using NGT's old analytical calculator for a stope with 100% CPB, the purple line is the binder content determined using Flac3D for a stope with 100% CPB (FOS of 2), and the green line is the binder content determined using Flac3D for the above PW design (FOS of ~2). The approximate failure surface plot is also shown in Figure 13, with the failure surface initiating at the top of the original plug, running through the bottom cylinder, and then along the interface of the WR cylinder and the CPB.

3.2 *As-Built*

PW operations in the 085A stope started on September 28th, 2019. There was a 1.5 day lag in WR deposition to account for the blasted rock chute material. The first truck used the rock

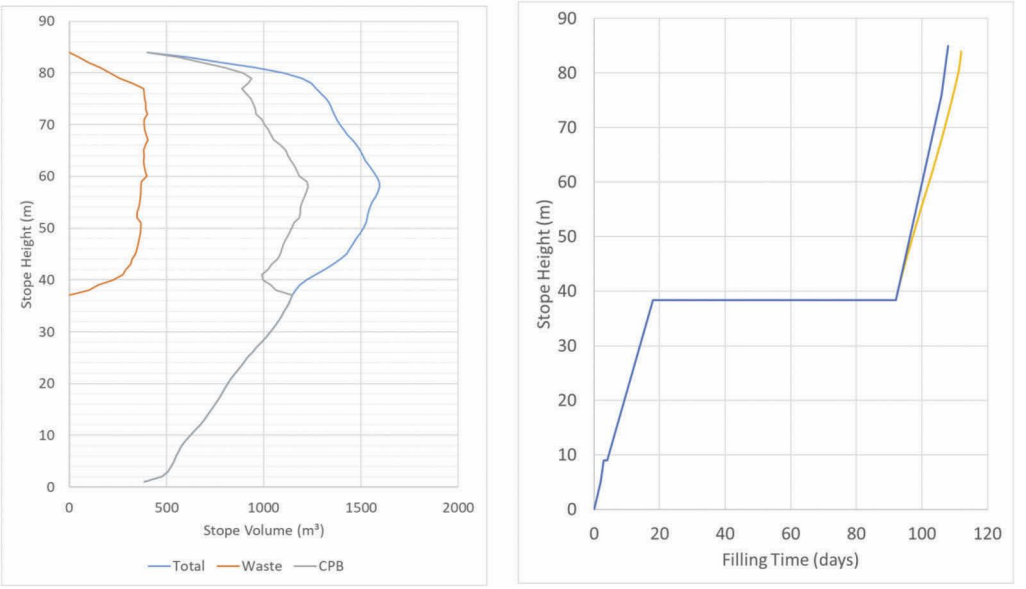

Figure 12. Graphs showing designed volume of CPB and WR within the stope and the estimated minimal stope filling time.

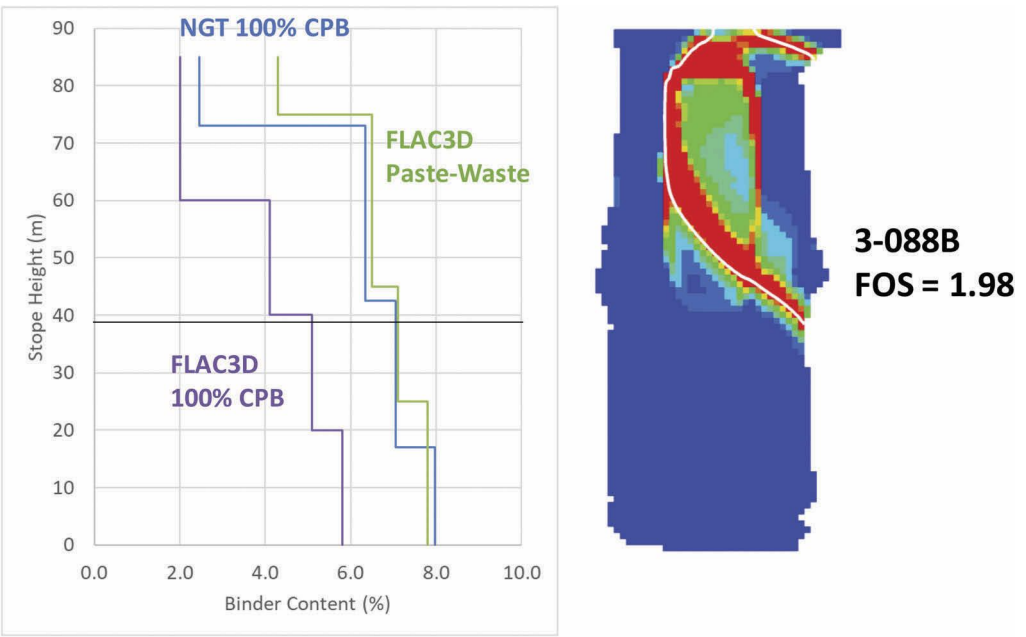

Figure 13. Graph comparing the design PW to 100% CPB binder contents and the modelled failure surface of the critical exposure.

chute on the September 30th, 2019. Figure 14 shows the cumulative gain of the PW material during the 085A pour. There are two distinct filling areas separated by a multi-day paste plant (PP) maintenance shutdown. There was a period just after the shutdown where limited WR

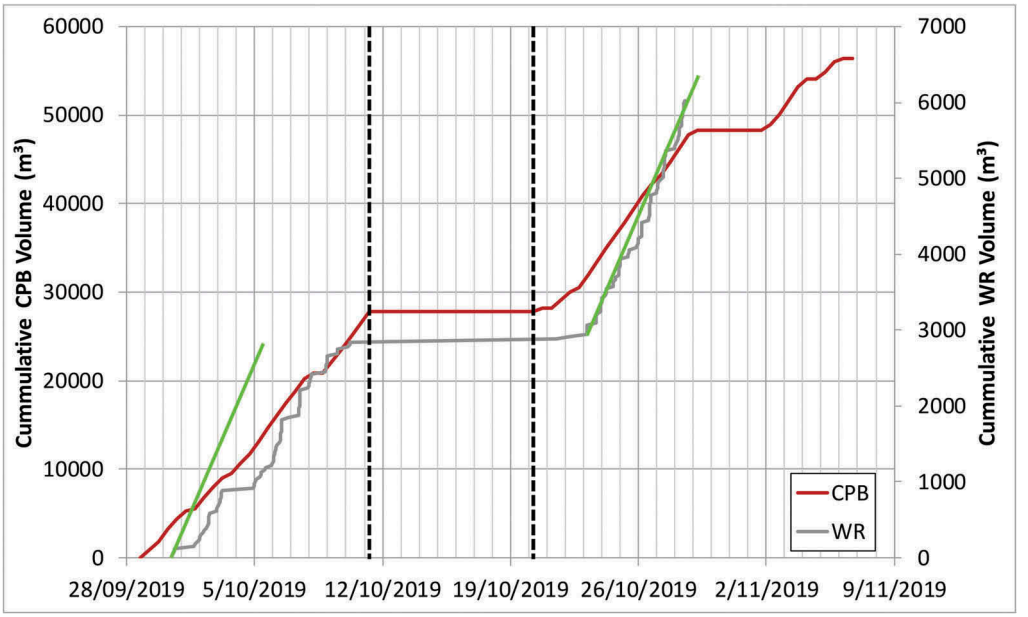

Figure 14. Cumulative depositional rates for CPB and WR into the 085A. The green lines are the maximum WR deposition rate allowed (12 trucks per shift).

was deposited. This was due to the rock chute's stop block being damaged and requiring repairs. The green lines show the design PW rate of 12 trucks per shift. A comparison of these lines to the actual deposition show that the WR placement rates, prior to the shutdown, were jagged and significantly below the design rate. Some of these were due to miscommunications between the paste plant operator and Mine Control resulting in the rock chute being closed even though the PP was operating. The WR deposition rates after the PP shutdown were much improved. This improvement was driven by the experience derived from the previous deposition and improved direction and communication between the stakeholders.

There were some interesting results that came out of the deposition rate monitoring. At DBS, truck movements are the responsibility of Mine Control (or Pitram). Prior to filling the 085A stope, it was anticipated that, given conversation with Mine Control, it would be easier to space the trucks over the shift. However, as observed in Figure 14, it rapidly became apparent that it was easier to dump several trucks over a short time period. In this way, the actual deposition patterns were closer to the 'instantaneous' model (discussed in Section 2.1.2) than the expected behaviour.

In order to monitor the pour, CMS were taken every couple of days while the stope was filling (Figure 15). The 'start of paste-waste' surface was taken after the plug was finished. The CMS taken on the September 30th was to determine if the rock chute material had been sufficiently covered prior to open the rock chute for WR deposition. There was no WR deposited between the 21st and the 23rd and this is shown in how the surfaces' shape change between CMSs taken on the 19th and the 23rd. The surfaces also show some interesting 'ponding' effects where flow of the CPB was modified by the WR cone.

Also shown in Figure 15 is the design and as-built WR cylinders. Note that the as-built was generated using the CMS surfaces and WR deposition log, and is intended to be a worst-case scenario. A spatial comparison shows good alignment between the design and the as-built in the north-south direction but a poor alignment in the east-west direction. For this particular stope, the alignment in the north-south direction was most important as this kept the WR material away from the exposed surfaces.

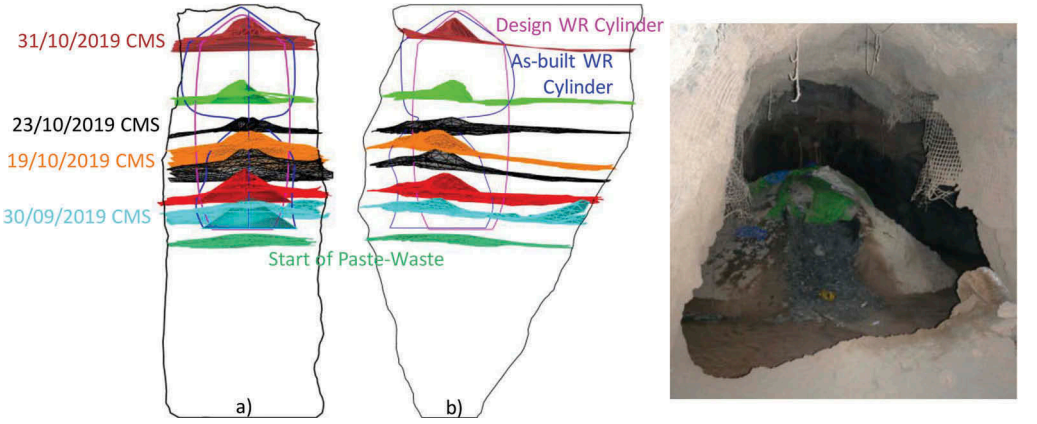

Figure 15. Cavity monitoring surveys taken during the pour with a) looking north, and b) looking west. The initial WR cylinder design shape (magenta) and the 'worst-case' as-built (dark blue) are also shown. Also shown is a photograph of the top of the stope taken on 31/10/2019.

However, it would be beneficial to know if the east-west alignment issues could be explained. To this end, a Trajec3D model was completed using the CMS of the rock chute as an approximate guide. The actual rock chute was not vertical but was slightly inclined towards the south. The results are shown in Figure 16, and show better correlation to WR cone locations than the original WR design shape (shown in magenta). However, some of the surfaces, particularly the 19/10/2019 CMS, do not match the Trajec3D analysis. This difference highlights the importance of tracking the backfill surface over the duration of the pour.

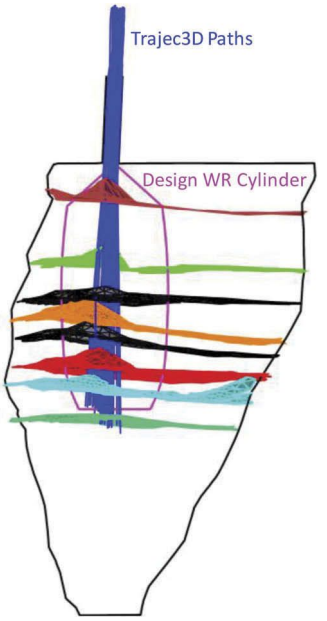

Figure 16. Traject3D model compared to the CMS surfaces obtained while filling the 085A and a photograph of the top of the stope after WR deposition finished.

Stability modelling is not usually redone unless there is an issue during pouring. In this case an erroneous calculation on the stope run sheet after the PP shutdown meant that the PP operator started the plant at a lower binder content. This mistake was eventually rectified but it meant there was a weak layer in the backfill. Therefore, a stability model was completed to identify if there were stability issues and to determine if additional binder was required in the upper portions of the stope. The results of this model are shown in Figure 17. Using the as-built WR cylinder shape, the FOS for the critical exposure models without a weak layer and with a weak layer were 2.09 and 2.00 respectively, meaning there was no stability issue.

There are two points of interest that come out of these stability models. The first was that the FOS of the non-PW model was higher than the design model. This was due to the decreased WR deposition during the first deposition phase. The other was that the failure surface, in the PS model, was shallower compared to the surface generated in Figure 13, due to the smaller size of the lower WR cylinder.

3.3 *Reconciliation*

A comparison of the original design and the as-built highlights the following:

- The original design called for a deposition of approximately 20,000 tonnes of WR. The actual amount of deposited WR was approximately 12,000 tonnes. There are several reasons for this, mainly the decreased WR deposition rates obtained prior to the shutdown and the time spent repairing the stop block.
- It was anticipated that PW would decrease the filling time by around 4 days. The actual decrease in time was about 3 days.
- The original design binder cost was approximately $345,000 more than the non-PW design (purple line versus green line in Figure 13). Normalizing this cost to the amount of WR deposited, the unit cost is around 12 $ binder per deposited WR tonne. The as-built results give a unit cost of 37 $/tonne.

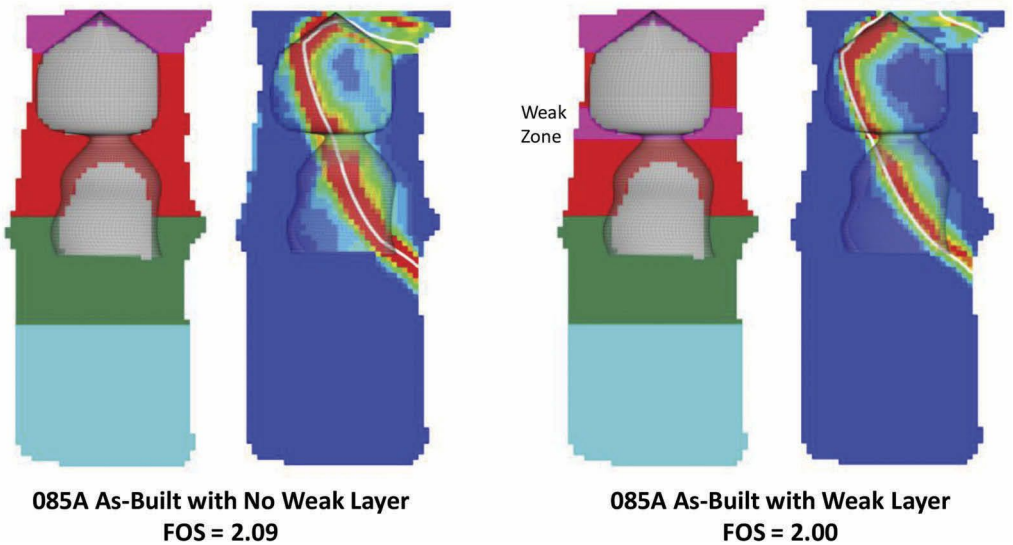

Figure 17. Stability model results comparing models with and without the weak CPB layer.

3.4 *Future work*

The 085A stope will continue to be monitored during the subsequent exposures. There are also plans to mine into the backfill along the mid-level drive in order to get an idea of the size of the halo and what it looks like. An attempt to obtain drill core from the fill mass will also be attempted dependent on drill availability.

4 CONCLUSIONS AND RECOMMENDATIONS

Due to the expansion of the DBS UG mine, there will be a WR surplus for the next 7 years, requiring this material to be transported and disposed of on surface. One of the mitigation measures, for reducing this surplus, was to increase the amount of PW being deposited UG by increasing the amount of in-stope WR deposition.

The first part of this paper presented a design methodology for designing a PW backfill mass that utilizes an encapsulation approach. Included in this methodology were discussions related to determining how the WR enters the stope, the approximate volume and shape of the encapsulated WR within the stope, and the stability of the backfill mass. The stability analysis also looked at how the modelling inputs were developed and utilized.

The second part of this paper was a case study dealing with the 085A stope, which was the first backfill mass designed using this methodology. Included in this case study was a monitoring program that allowed the design to be compared to how the stope was actually filled.

The design was relatively complicated due to multiple, large exposures on two sides and limited access to the stope (due to the southern wall overbreak). This limited the amount of WR that could be deposited.

The CMS taken of the stope and the deposited material logs maintained while it was filled allowed for an as-built of the stope to be created. There were several notable deviations from the design:

- The depositional surfaces generated from the CMS showed that the WR surfaces migrated southwards during filling.
- The first was that there was significantly less WR deposited. The main reasons for this were the rock chute closure while the stop block was repaired and the slower initial WR deposition rate. The deposition rate improved during the later stages of the stope filling.
- The second was that a weak CPB layer was poured due to a mistake made at the paste plant. The impact of this weak layer was analysed by using the stability modelling methodology presented in this paper and it was found that the weak layer did not reduce the stability FOS below the site standard.

In general, the response to this initial trial has been positive and additional stopes are being identified and ranked as PW targets. Future work is also planned for the 085A which includes monitoring the future exposures and obtaining samples from the CPB and WR halo zones.

ACKNOWLEDGEMENTS

The Authors would like to acknowledge the help of the DBS Pitram Operators, Adam Zajac, and Ceinwen Mackay in collection the data used in this paper. The Authors also acknowledge the Newmont Goldcorp Tanami Management Team for their support in the writing of this paper.

BIBLIOGRAPHY

BasRock. 2019, '*Trajec3D. Version 1.7.2.3'*. BasRock, Perth, WA, Australia.

Basson et. al. 2015 – Basson, F.R.P., Dalton, N.J, Barsanti, B.J, and Flemmer, A.L. 2015. Simulate waste rock flow during co-disposal for dilution control. [In:] *Proceedings of Design Methods in Underground Mining*. Perth: ACG.

Deswik. 2019, '*Deswik.CAD. Version 2017.1'*. Deswik, Brisbane, QLD, Australia.

Itasca Consulting Group, Inc. 2019, '*FLAC3D: Fast Lagrangian Analysis of Continua in 3 Dimensions. Version 6.0'*. ICG, Minneapolis MN, USA.

Veenstra, R.L. 2019. *Flac3D FOS Solver Calibration to Tanami Stopes*. Newmont Goldcorp Australia: Internal Communication.